Identification of plant species in an alpine steppe of Northern Tibet using close-range hyperspectral imagery

Enqin Liu [a], Hui Zhao [b,*], Shuhui Zhang [a], Jing He [a], Xin Yang [a], Xiangming Xiao [c]

[a] *College of Earth Sciences, Chengdu University of Technology, Chengdu, Sichuan 610059, China*
[b] *Institute of Mountain Hazards and Environment, Chinese Academy of Sciences, Chengdu, Sichuan 610041, China*
[c] *Department of Microbiology and Plant Biology, University of Oklahoma, Norman, OK 73019, USA*

ABSTRACT

The identification of plant species in alpine steppes of Northern Tibet is of great significance for revealing community structures and for monitoring vegetation degradation and restoration from remote sensing images. Plants in the alpine steppe of Northern Tibet are short, sparse, and highly heterogeneous in spatial distribution. This peculiarity makes the plant species identification here much more difficult than the identification of plants with high spatial homogeneity. We aimed to explore the potential of close-range hyperspectral imaging for plant species identification in alpine steppe under field conditions. Specifically, we assessed which spectral bands are effective and which classification methods are suitable for plant species identification. A close-range hyperspectral image of grassland in Nagqu, Tibet were acquired in August 2018. Four methods, including derivatives, continuum removal, spectral indices, and principal components were used to enhance the differences in spectral characteristics between plant species. Then, two band selection methods, including Mahalanobis distance and variable importance evaluations based on a random forest (RF) were used to reduce dimensionality and select indicators beneficial for identifying grass species. Four datasets were constructed based on those indicators and were used as the input data for four classifiers, support vector machine (SVM), RF, artificial neural network (ANN), and spectral angle mapper (SAM). We found that (1) bands selected using Mahalanobis distance and variable importance evaluation method showed that the red bands, red edge bands, and spectral indices were important for plant species identification; (2) among the four classifiers, the ANN classifier had the highest overall classification accuracy on Dataset 3 of the reflectance images, which was 94.73%, and the Kappa coefficient was 0.93; (3) the machine learning algorithms RF and ANN performed well for identifying plant species, with an overall accuracy more than 91.59% and kappa coefficient above 0.89. These results suggest that close-range hyperspectral image and machine-learning classifiers, such as RF and ANN, can be used to effectively identify plant species in alpine steppe.

1. Introduction

Alpine steppe forms two-thirds of the total area of Tibetan Plateau (TP) and is one of the world's most important ecosystems (Cui and Graf 2009; Yao et al. 2019). It not only performs important ecological functions such as climate control, water conservation regulation, biodiversity conservation, wind and sand fixation, and carbon storage at a global scale (Sun et al. 2019), but it also provides critical ecosystem services, such as pastoral production, cultural inheritance, tourism, and recreation at local and regional scales (Dong et al. 2020). Located in the hinterland of the TP, the Northern Tibet alpine steppe serves as a major

ecological security barrier and a special livestock farming base in the plateau (Liu et al. 2013; Kemp et al. 2013). Alpine steppe is sensitive to climate warming and anthropogenic activities (Chen et al. 2014a).

Since the 1980s, under the combined effects of climate change and unreasonable human activities such as overgrazing, alpine grassland on the Tibetan Plateau has undergone considerable degradation (Lehnert et al. 2013). Grassland degradation creates structural imbalances in vegetation communities, leading to native plant species extinction and noxious weeds invasion. A series of measures have been adopted to restore grassland ecology on TP, including fence enclosures, grazing management, cultivated grassland, and rodent pest control (Harris et al.

Table 1

Remote sensing instruments commonly used for plant species detection and monitoring.

Sensor types	Instruments	Publications
In-situ point sensor	e.g. ASD, HR1024	Cushnahan et al. 2016; Deng et al. 2019
In-situ imaging sensor	e.g. Crane-mounted hyperspectral imaging sensor	Monteiro et al. 2008
Airborne Spectrographic Imager	e.g. CASI, AISA-Eagle, HySpex images	Mansour et al. 2012; Kopeć et al. 2019; Sabat-Tomala et al. 2020
Spaceborne Spectrographic Imager	e.g. HJ-1A/HSI	Ai et al. 2020
LiDAR	e.g. Leica ALS70 LiDAR system	Fisher et al. 2018
UAV with multi-spectral imaging spectrometer	e.g. Tarot T15 Octorotor with a modified Canon camera	Lu and He 2017
UAV with hyperspectral imaging spectrometer	e.g. DJI Matrice 600 with LCTF imaging camera	Ishida et al. 2018

2016; Zhao et al. 2018; Yao et al. 2019). The TP covers a vast area and is characterized by extreme weather patterns. Manual grassland degradation monitoring and ecological restoration on TP are currently inefficient and highly labor intensive.

Plant species identification is a classic and hot issue (Xiao et al. 2018). If remote sensing images can be used to identify grass species, it can also be used to develop important grassland community structure indices, such as those for dominant grassland community species and community species compositions, which is of great significance for the regional scale monitoring of grassland degradation and ecological restoration.

The plant species identification on TP is affected by special weather conditions and vegetation characteristics. Cold weather conditions, short plant growth seasons (Ma et al. 2016), and high financial costs of experiments make it difficult to collect hyperspectral data. Vegetation grows well in July and August when temperatures relatively warm, but this period also coincides with the rainy season. Thus, suitable periods for hyperspectral data acquisition are short. Also, the alpine steppe is sparse (Ding et al. 2013), plants are short and heterogeneous, and canopy spectral characteristics are easily disturbed by soil under the grass. Therefore, the identification of plant species requires the use of remote sensing sensors of high spectral and spatial resolutions. So, it is difficult to identify different plant species using low- and medium-resolution remote sensing images, including hyperspectral images of low spatial resolutions. Due to the limitations of hyperspectral image acquisition, plant species on TP have not been identified at the level of individuals using remote sensing images.

It was recently found that hyperspectral sensor outputs offer considerable information on nutrient content and species compositions (Cushnahan et al. 2016). Their narrow bands reveal rich spectral differences between plant species. In addition, data sources such as unmanned aerial vehicles (UAVs) and LiDAR images provide more opportunities for plant species identification. Remote sensing tools commonly used for plant species identification are shown in Table 1. Remote sensing data required to study spatially homogeneous grasslands are considerably different from those required to identify spatially heterogeneous short grasslands. For plant species identification of homogeneous grasslands, satisfactory accuracy can be achieved by using airborne hyperspectral images (Mansour et al. 2012; Kopeć et al. 2019), UAV multispectral data (Lu and He 2017), or LiDAR images (Fisher et al. 2018). But plant species identification for heterogeneous grasslands is more difficult than homogeneous grasslands and need to use hyperspectral images with higher spatial resolution.

In identifying heterogeneous short plant species, previous research has mainly focused on the use of ground-based, non-imaging
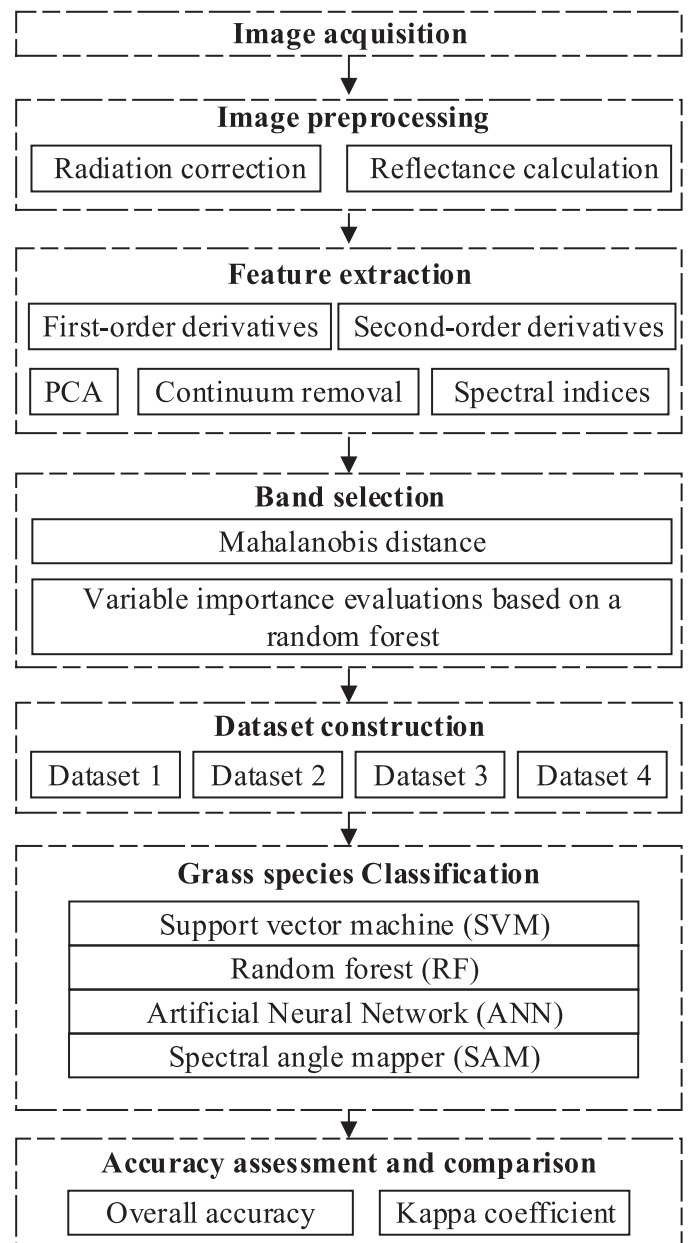

Fig. 1. Flowchart of plant species identification using close-range hyperspectral imagery.

spectroscopy (e.g. ASD) to analyze spectral features at the leaf scale and the determination of which sensitive bands are conducive to species differentiation (Cushnahan et al. 2016; Liu et al. 2013). These works provide useful theoretical explorations for plant species identification. But there is still a long way to identify heterogeneous short plant species from remote sensing images. A close-range imaging spectrometer can acquire hyperspectral images of grasslands under natural conditions when a hyperspectral sensor is mounted at a certain height above ground (e.g. 1–1.5 m) (Mishra et al. 2017). Close-range hyperspectral images have been used for identifying mangrove species (Cao et al., 2018) and plant species in mixed grassland communities (Lopatin et al. 2017). It was shown that close-range hyperspectral imagery has the potential for plant species identification. However, the use of close-range hyperspectral imagery for classification of alpine plant species under field conditions has not been reported. Considering the characteristics and importance of alpine grassland plants, it is necessary to explore the application of close-range hyperspectral imagery for
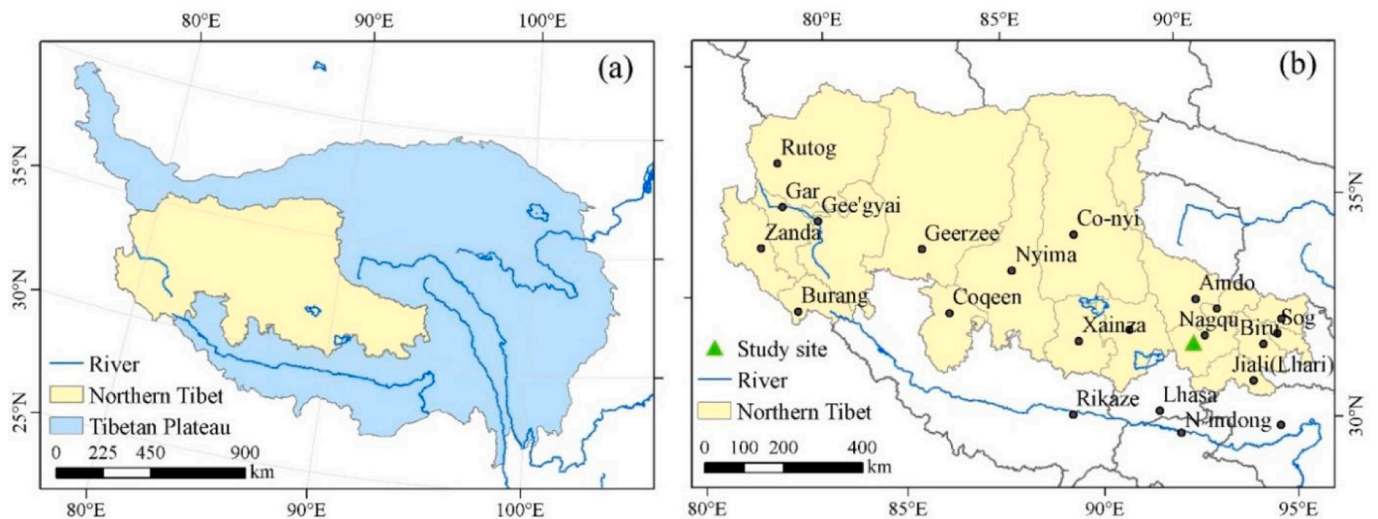
Fig. 2. Study area. (a) The location of Northern Tibet in the Tibetan Plateau. (b) the location of Study site.

identifying alpine plants species as a basis for further work to identify alpine plants species at a larger scale.

Our aim was to evaluate the application of close-range hyperspectral imagery in identification of alpine grass species under field conditions.

Our objectives were to clarify the following questions: (1) is close-range hyperspectral imagery applicable to the identification of alpine grassland species; (2) what are the differences in spectral characteristics between different species of alpine vegetation; (3) what spectral bands or

(c) *Kobresia humilis*

(d) *Leontopodium pusillum*

(e) *Potentilla saundersiana*
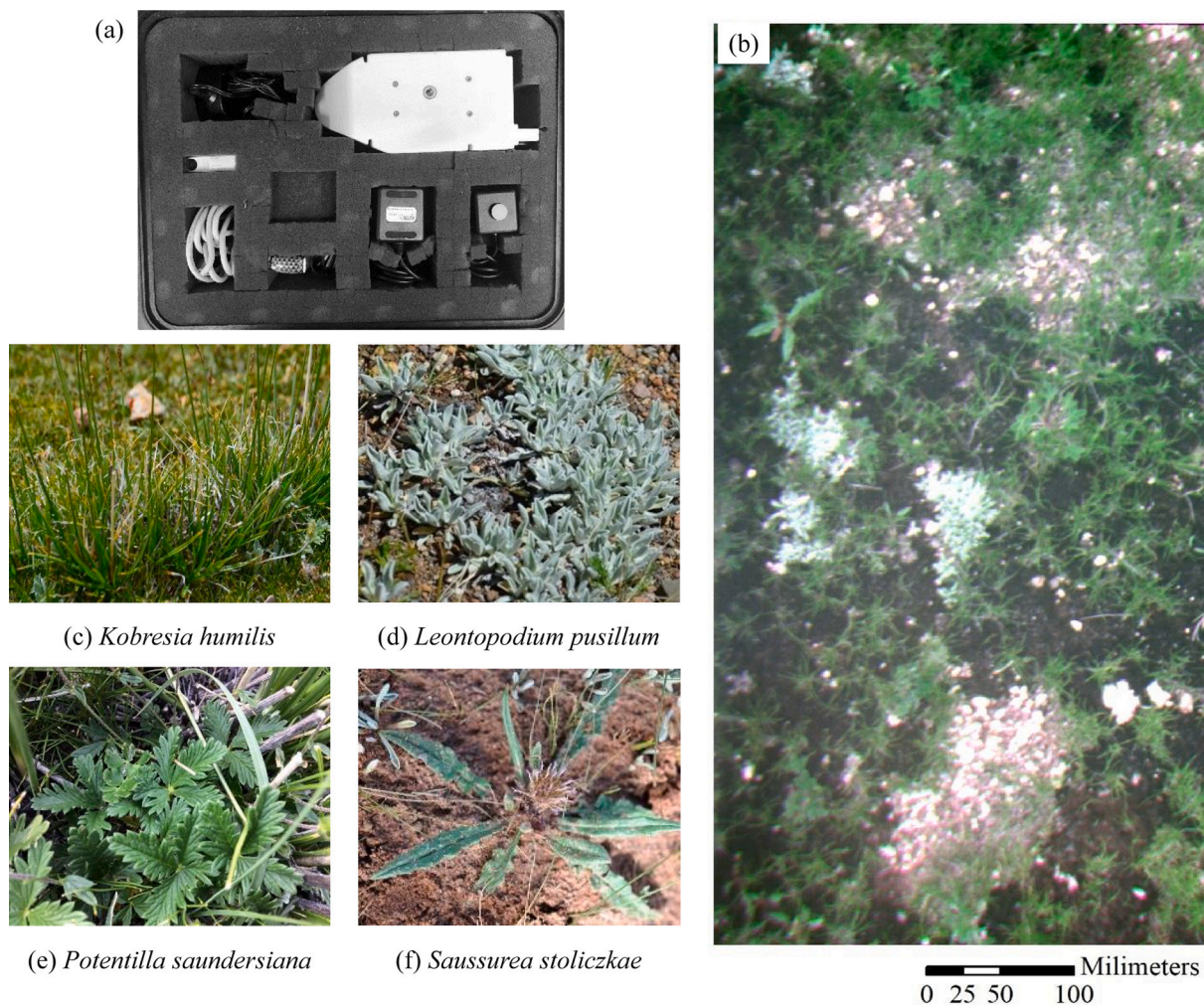
(f) *Saussurea stoliczkae*

Fig. 3. Spectrometer, close-range hyperspectral imagery, and field photos of plants. (a) The Rikola hyperspectral camera. (b) close-range hyperspectral imagery of a 0.65 mm spatial resolution of the study site. (c), (d), (e), and (f) are photos of plants in the field.

indices favor the distinction of alpine vegetation; and (4) which classifier is more effective in identifying vegetation species?

First, we acquired a close-range hyperspectral remote sensing image of degraded alpine grassland in Naqu. Second, multiple feature variables, such as spectral indices, were obtained by spectral feature transformation and operation to enhance differences in spectral characteristics between plant species. Third, the Mahalanobis distance method and variable importance assessment based on the RF algorithm were used to select spectral bands and indices favorable for plant species identification. Then, four datasets were established to compare the effectiveness of the selected bands for plant species classification. Finally, we used four classifiers for classification and accuracy comparisons. Our objective was to explore ways of identifying plant species in alpine degraded grasslands based on close-range hyperspectral images. The workflow of the plant species identification is summarized in Fig. 1.

2. Materials and methods

2.1. Study area

Our study area was in Nagqu, Northern Tibet (Fig. 2), China. The plateau has a subfrigid monsoon semihumid climate. The climate of the Northern Tibet Plateau is cold, presenting an average annual temperature of 0.1 °C for several years. The hottest temperatures in Northern Tibet occur in July with an average temperature of 10.0 °C while January is the coldest month with an average temperature of −11.2 °C (Chu et al. 2007). July and August are optimal months for vegetation growth.

Nagqu includes the largest pastoral area found in Tibet with grassland here accounting for 34.3% of the total grassland area in Tibet (Chen et al. 2014b). The grassland community in Nagqu has a simple species composition, a simple community structure, and a fragile ecosystem.

2.2. Hyperspectral image acquisition and preprocessing

We used the Rikola hyperspectral camera (Fig. 3(a)) developed by the Senop company of Finland to obtain a hyperspectral image of sparse alpine grasslands. The image includes 39 bands of 10 nm spectral resolutions ranging from 450 nm to 950 nm. Since the instantaneous field of view of the spectrometer was fixed at 36.5°, the image size and spatial resolution of close-range hyperspectral imagery were determined using the height of the instrument above the ground. The further from the ground, the larger the corresponding surface area and the coarser the spatial resolution. During the image acquisitions, the instrument was fixed at a height of 1 m above the ground with the camera being at a near-vertical viewing direction to the ground. The spatial resolution of the hyperspectral image was 0.65 mm, and the image footprint was 0.67 m × 0.67 m. The image covered the four main grass species in this area. A whiteboard was placed as a reference during imaging while dark current data were acquired from the instrument.

The image was acquired at noon on August 3, 2018. Dark current data were acquired and used to perform radiation correction and obtain a radiation image. We selected 400 whiteboard pixels from the map to calculate their average radiation value. Then, the radiance image was converted into a reflectance image based on the reflectance of the whiteboard. The reflectance of the whiteboard was provided by Senop. Then, the whiteboard section of the image was removed to obtain the final hyperspectral reflectance image of grassland shown in Fig. 3(b). The image included a total of 494,915 pixels with 515 columns and 961 rows. The coverage area was 0.21 square meters. Although a single image cannot cover all grass species in northern Tibet, the grass species in this image have characteristics common of grasses on the TP, such as sparseness and shortness. Therefore, this close-range hyperspectral image is representative of the landcover.

Table 2
Selected spectral indices for grass classification. Rx denotes the reflectance at wavelength x nm.

Spectral indices	Formula	References
Normalized difference vegetation index (NDVI)	$(R_{804} - R_{654})/ (R_{804} + R_{654})$	Rouse et al. 1974; (Tucker, 1978)
Simple ratio index1(SR1)	R_{800}/R_{675}	Jordan 1969; Blackburn 1998
photochemical reflectance index (PRI)	$(R_{570-531})/ (R_{570}R_{531})$	(Gamon et al., 1997)
Triangular Vegetation Index (TVI)	$(120 (R_{750}-R_{550})-200 (R_{670}-R_{550}))/2$	Broge and Leblanc 2001
Simple ratio index2(SR2)	$R750/R700$	Lichtenthaler et al. 1996

2.3. Feature extraction

2.3.1. First-order, second-order derivatives, and continuum removal

Hyperspectral data are rich in spectral information, which allows for the accurate identification of plant species but also generates a considerable amount of redundant data. As the spectral reflectance of multiple plant species are also often very similar, we needed to enhance the differences between the spectral characteristics (e.g. spectral reflection or absorption characteristics) between plant species and reduce the amount of data that was useless for plant species identification.

We employed first- and second-order derivative and continuum removal methods to enhance differences between plant species. Spectral differential transformation is one of the most used feature analysis methods for hyperspectral remote sensing data (e.g. first- and second-order derivatives). Many studies have shown that a derivative spectrum can reduce low-frequency background noise and the influence of the atmosphere (Zhang et al. 2014; Cui et al. 2019). Spectral differentiation is widely used for tree species identification (Xu et al. 2019) and crop disease. In addition, due to the effectiveness of analyzing and intensifying the spectral characteristics in vegetation, continuum removal has been widely used to estimate leaf area indices, crop varieties, and vegetation diseases (Luo et al. 2019; Izzuddin et al. 2018).

2.3.2. Spectral indices derived from hyperspectral images

Spectral indices are effective and simple algorithms for the quantitative analysis of vegetation properties and involve using certain bands of hyperspectral data to perform various mathematical calculations to obtain meaningful values.

Hyperspectral sensors generate better vegetation classification results than multispectral sensors, and their narrow bands allow for the selection of bands and the creation of narrowband indices for a range of biophysical and biochemical properties (Cushnahan et al. 2016). A number of spectral indices have been developed to detect and map the following three vegetation properties: (1) structural properties, including fractional cover (Gao et al. 2020), green leaf biomass (Celleri et al. 2019), leaf area indices (LAIs) (Broge and Leblanc 2001; Din et al. 2017), and FPAR (Tan et al. 2018) canopy biochemical properties, including water (Pasqualotto et al. 2018), plant chlorophyll content (Liang et al. 2016; Liu et al., 2015), and N, P, and K content in crops (Din et al. 2017; Lu et al. 2019); and (3) plant physiological stress (Zhang and Zhou 2019; Feng et al. 2017).

Spectral indices are widely adopted to assess and monitor biophysical and biochemical vegetation states, which is helpful for agricultural applications such as the management of crop nutrition and growth for agriculture (Huete 2012). Many academic publications show that SR, NDVI, PRI, and TVI spectral indices effectively predict vegetation structure parameters such as the LAI and fractional cover(Prasad, 2011) and track changes in plant physiology associated with photosynthetic efficiency (Gamon and Surfus 1997; Cushnahan et al. 2016). In this study, we extracted PRI, TVI, SR1, NDVI, and SR2 spectral indices for the classification of plant species. The formulas of these spectral indices are

shown in Table 2.

2.3.3. Principal components of hyperspectral images

Principal component analysis (PCA) is a technique used to emphasize variations and reveal strong patterns in a dataset (Arsa et al. 2018). The principal component transformation of hyperspectral images can maximize the amount of effective information in data and reduce data dimensions. We performed principal component transformation on 39 reflectance spectral bands. The first principal component was retained for classification because it had the largest variance and retained the most information of the original data.

2.3.4. In situ sample data

From photos in the book "Atlas of Rangeland Plants in Tibet", we found four plant species in the hyperspectral image: *Kobresia humilis* (Fig. 3(c)), *Leontopodium pusillum* (Fig. 3(d)), *Potentilla saundersiana* (Fig. 3(e)), and *Saussurea stoliczkae* (Fig. 3(f)). Among them, *Kobresia humilis* is the dominant species (excellent forage), *Potentilla saundersiana* and *Saussurea stoliczkae* are associated species, and *Leontopodium pusillum* is a degenerative indicator grass of the TP alpine steppe. The grasses are about 2–20 cm tall with narrow leaves. The image also contains soil and stones. Thus, 6 types of objects are shown in the hyperspectral image. Photos taken by camera were used as the basis for selecting samples from the hyperspectral image.

2.3.5. Statistic analyses for the spectral characterization of plant species, soil, and stones

It has been found that different plant species have significantly different spectral curve characteristics (Schmidt and Skidmore 2001). Spectral differences form the basis for plant species identification. Due to their high spatial resolution, the leaves of different types of grass are clearly shown on the close-range hyperspectral image, which is beneficial for selecting pure pixels.

Using the field photos as a reference, we selected 32,352 pixels from the hyperspectral image and used them as samples to calculate the mean spectral reflectance, mean first-order derivative, mean second-order derivative, and mean continuum removal spectra of six kinds of objects. We used 10,155, 3372, 847, 6304, 6358, and 5316 pixels as training samples for *Kobresia humilis, Potentilla saundersiana, Saussurea stoliczkae, Leontopodium pusillum*, soil, and stones, respectively. Then, we analyzed the spectral characterizations of the plant species, soils, and stones based on the differences we observed.

2.4. Image classification for plant species, soil, and stones

We identified plant species using four steps: (1) input image preparation; (2) training data collection; (3) algorithm application for classification; and (4) map accuracy assessment.

2.4.1. Input images

As high spatial and spectral resolution generate large amounts of data, calculations, and storage, we selected effective bands using the Mahalanobis distance method and variable importance assessment based on the RF algorithm to compress the data as much as possible while maintaining effective information for vegetation recognition.

To compare the effectiveness of the selected bands for classification, we established four datasets for plant species identification. Dataset 2 includes bands selected based on the Mahalanobis distance combined with PC1 and five vegetation spectral indices. Dataset 1 is composed of bands selected from Dataset 2 via variable importance evaluation based on random forests. Dataset 3 is composed of reflectance data with 39 bands. All unfiltered reflectance images, first derivative images, second derivative images, continuum removal images, PC1 data, and the five vegetation spectral indices were used to construct the fourth dataset with a total of 171 bands.

(1) Band selection based on Mahalanobis distance

Large data volumes and redundant information are common problems encountered in the field of hyperspectral target recognition (Qu and Liu 2017). Multi-feature information extracted from hyperspectral data includes both information useful for plant species recognition and large amounts of redundant information. The vast amount of data that hyperspectral sensors gather introduces so many dimensions that accuracy levels can be hindered rather than improved (Hughes and Gordon 1968; Pal and Giles 2010). As not all features are helpful for classification, we selected bands beneficial for distinguishing plant species from a large collection of data using feature selection methods and then constructed the dataset used for classification.

Mahalanobis distance was first coined by Indian statistician Mahalanobis (Mahalanobis, 1936). It is an efficient tool for identifying differences between various vectors and has been successfully applied for tree and crop species recognition and hyperspectral anomaly detection (Zhang et al. 2015; Zhao et al. 2018). If an outlier follows a chi-square distribution (Brereton and Richard 2015), a critical value is of 0.01 significance level with 2 degrees of freedom and 99% confidence. An observation can be considered extreme when its Mahalanobis distance exceeds 9.21 (Atkinsonand Marco 2014).

(2) Band selection based on variable importance evaluation

We used a variable importance evaluation based on the RF algorithm to filter features with strong impacts on plant species recognition. The multivariate feature importance measure of the RF model has been extensively exploited in different scenarios, including to reduce the number of dimensions in hyperspectral data and identify the most relevant multisource remote sensing and geographic data (Belgiu and Lucian 2016). It uses bootstrapping with sampling to select n samples from the sample set as a training set and then trains and generates a decision tree using the training set obtained from sampling. m training sets then generate m decision trees and individually evaluate how much each variable contributes to every decision tree in the random forest averaged over all trees to measure the importance of each variable in the random forest (Menze et al. 2009). Then, a small subset of 'strong variables' is used for classification.

2.4.2. Collection of training data for algorithms

The same samples described in Section 2.3.5 were used to train classifiers.

2.4.3. Classifiers for plant species identification

Classification is central to plant species identification and should comprehensively utilize multiple data sources and process high-dimensional data. Support vector machine (SVM), random forest (RF), and artificial neural network (ANN) approaches are forms of supervised machine learning and are widely used for vegetation classification using hyperspectral imagery (Ai et al. 2020; Sabat-Tomala, 2020, Amlekar and Gaikwad 2019). Spectral angle mapper is a commonly used method of hyperspectral image classification. To identify classifiers suitable for the classification of plant species shown in hyperspectral images, four classifiers were employed to classify the above four datasets.

(1) Support vector machine (SVM)

SVM is based on statistical learning theory. It maps linear indivisible samples of low-dimensional input space to a high-dimensional space by a linear mapping algorithm to make them linearly separable (Wang et al. 2018). The SVM kernel function plays a vital role in its performance. Radial basis function, linear kernel function, and sigmoid kernel function are commonly used kernel functions. Here, we chose the radial basis function for its efficiency and smaller number of computational difficulties (Sabat-Tomala et al. 2020).
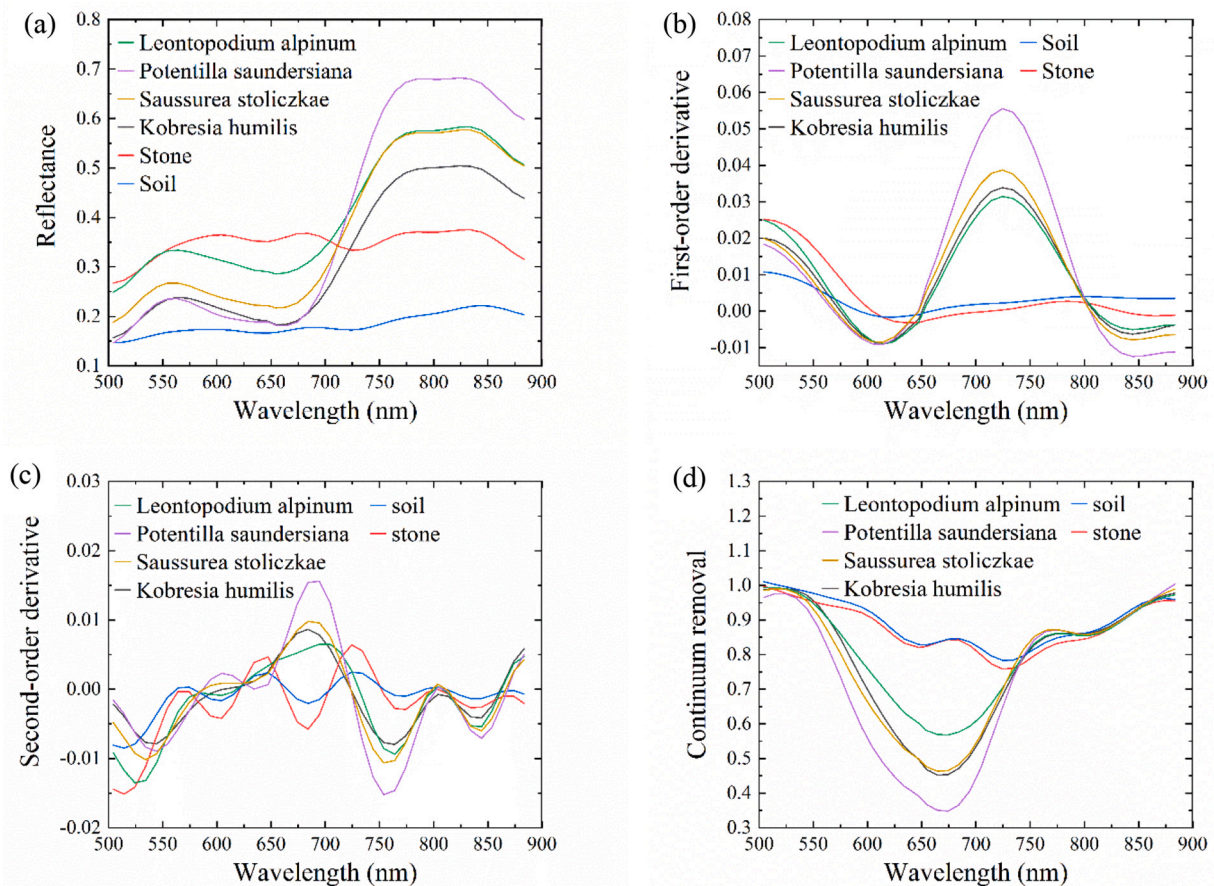
Fig. 4. Spectral characteristic curves of the four plant species. (a) the reflectance curves, (b) the first-order derivative spectral curves, (c) the second-order derivative spectral curves, and (d) continuum removal spectral curves.

(2) Random forest (RF)

The RF classifier is an ensemble classifier that produces multiple decision trees from a randomly selected subset of training samples and variables (Belgiu and Lucian 2016), and the classification results are based on scores obtained by voting with multiple classification trees. The RF classification model is sensitive to the impact of the number of trees and the number of variables chosen to grow the tree (Zakrani et al., 2019). Refer to the research results of Liu et al. (2013), the number of trees was set to 100 in this case. The number of variables was set to the square root of the total number of feature variables.

(3) Artificial Neural Network (ANN)

Scholars have developed various forms of neural network models and algorithms, such as convolutional neural network (CNN), feedforward neural network (FNN), and Kohonen self-organizing network (SOM). A Multilayer perceptron (MLP) is one of the representative feedforward neural network models and ensures high recognition accuracy when performing robust training (Driss et al. 2017). Rectified linear unit (ReLU) is the most successful and commonly used activation function in neural networks. We adopted an MLP neural network model with ReLU activation function for our study.

(4) Spectral angle mapper (SAM)

SAM is a measurement method based on the similarity of spectral dimension curves. The algorithm determines the spectral similarity between two spectra by calculating the angle between the spectra, treating them as vectors in a space with dimensionality equal to the number of

bands (Kuching 2007). A smaller angle indicates a higher degree of matching with the reference spectrum. Many of our experiments indicated a relatively good classification effect is achieved when the angle was set to 0.3. When the angle was higher than 0.3, there was no significant improvement in the classification result, so the maximum angle threshold was set to 0.3.

2.4.4. Map accuracy assessment

Using the field photos as a reference, another 35,300 pixels of sample data for the six types of objects were collected from the hyperspectral images for accuracy verification. Training samples and testing samples were different data, and they were independent of each other. The testing samples of *Kobresia humilis, Potentilla saundersiana, Saussurea stoliczkae, Leontopodium pusillum*, soil, and stones were 5291, 6164, 1127, 6759, 10,530, and 5429 pixels, respectively. We use those samples as ground truth regions of interest (ROIs) to verify the accuracy of our classification results. The classification results of the four datasets were based on the same validation samples used for accuracy evaluation. Overall accuracy (OA) and kappa coefficient values are used to evaluate the accuracy of plant species identification.

3. Results

3.1. Spectral characteristics of plant species, soil, and stones

As shown in Fig. 4(a), the reflectance of soil was significantly lower than the spectral reflectance of vegetation and stone at 450–900 nm, and thus vegetation and soil could be easily distinguished according to the spectral difference. Stone had the highest reflectance at a range of 594–630 nm and was significantly different from vegetation in the near-
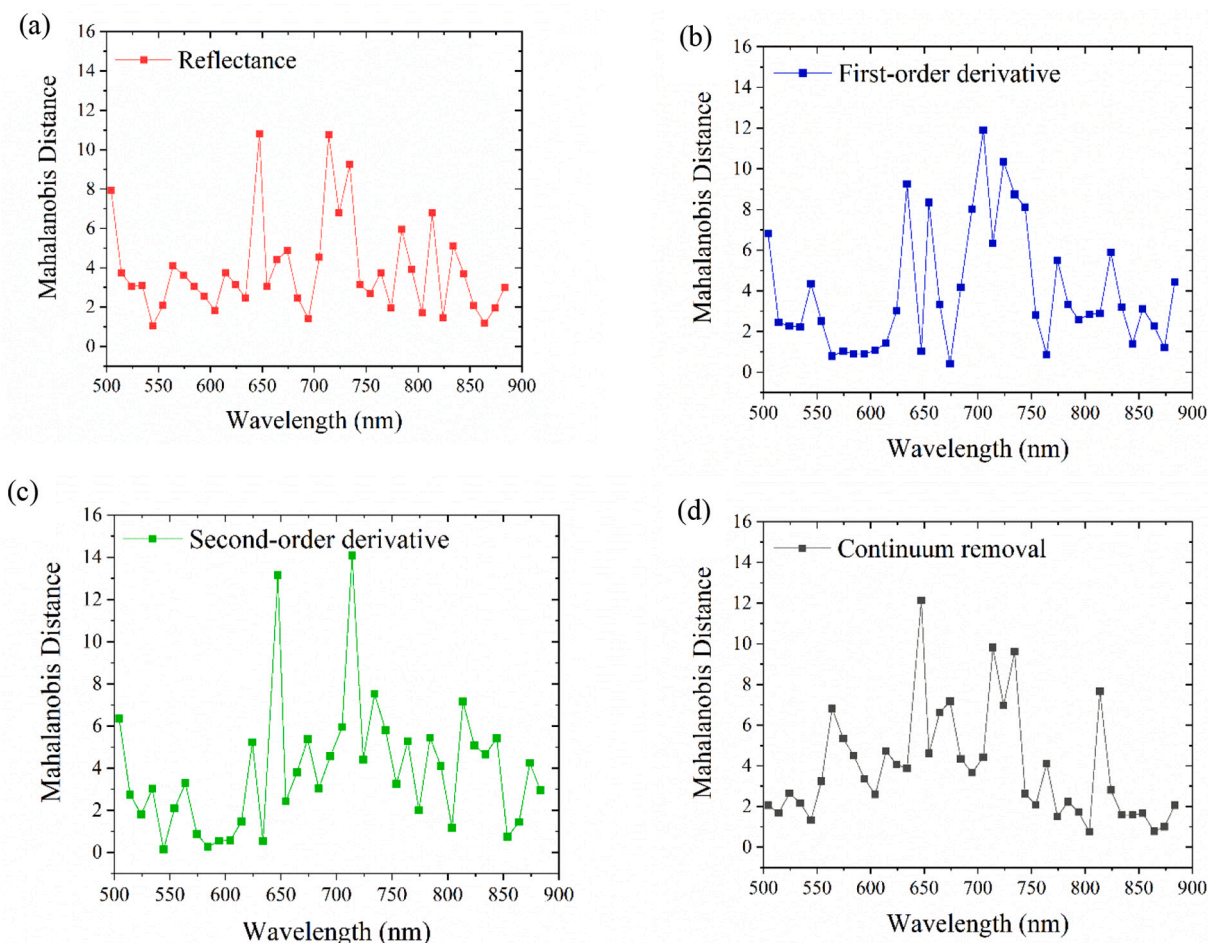
Fig. 5. Mahalanobis distance between four plant species. (a), (b), (c), and (d) are the Mahalanobis distance between plant species based on the reflectance images, first-order derivative spectra, second-order derivative spectra, and the continuum removal spectra, respectively.

Table 3
Spectral features selected via Mahalanobis distance analysis based on original spectra, first-order derivative spectra, second-order derivative spectra, and continuum removal spectra.

Band types	Wavelength (nm)	Mahalanobis distance	Number of bands
Reflectance	647,714,734	10.81, 10.74, and 9.24	3
First-order derivative spectral	634,704,724	9.24, 11.9, and 10.34	3
Second-order derivative spectral	647,714	13.17 and 14.10	2
Continuum removal spectral	647,714,734	12.13, 9.81, 9.61	3

infrared band. Thus, it is also easy to distinguish between stone and vegetation. However, the spectral curves of the different plant species were similar and easy to confuse. For example, the spectral reflectances of *Kobresia humilis* and *Potentilla saundersiana* were similar within the visible band while those of *Leontopodium pusillum* and *Saussurea stoliczkae* were similar within the near infrared band. The spectra of all four plant species had steep slopes in the range of 680–750 nm.

Fig. 4(b) shows that the first-order derivative values of the four plant species were higher than those of soil and stone at 600–820 nm. Within this wavelength range, *Potentilla angustifolia* had the highest first derivative value, and soil and stone had much lower values than grasses. Fig. 4(c) shows that the difference between the second-order derivative values of the six objects was not as obvious as the difference between the

spectral reflectance and first-order derivative values. Spectral difference bands were as follows: 624 nm, 644–674 nm, 694 nm, 714 nm, 744 nm, 764 nm, 784 nm, and 814–844 nm. Fig. 4(d) shows that variations in the continuum removal spectral values of the four plant species were considerable at 520–730 nm, with values for stones and soil significantly higher than those of grass, and with values for the four plant species being low and having pronounced differences between them.

3.2. Selection of spectral bands for image classification

The Mahalanobis distance of the four typical plant species based on the reflectance, first-order derivative spectra, second-order derivative spectra, and continuum removal spectra were separately calculated (Fig. 5(a), Fig. 5(b), 5(c) and 5(d), respectively). Bands with Mahalanobis distance exceeding 9.21 were selected as shown in Table 3. The 11 bands selected based on the Mahalanobis distance together with PC1 and five spectral indices (5 bands) totaled 17 bands, which constituted Dataset 2. We employed the variable importance evaluation based on the RF model to select bands from Dataset 2 because it had many bands. The results of the importance evaluation are shown in Table 4. Reflectance (647 nm), PCA1, and SR2 were the top three indicators for grass species identification based on the variable importance evaluation method. The first ten bands in Table 4 were used to construct Dataset 1, as these ten bands contributed to about 90% of the classification results.

Here, we used a total of six types of data sources, namely reflectance, first-order derivatives, second-order derivatives, continuum removal, principal component transformation, and spectral indices. To facilitate our understanding of different variables, we selected one variable for

Table 4
Evaluating the importance of variables by the RF algorithm.

No	Variables name	Variables importance	No	Variables name	Variables importance
1	Reflectance (647 nm)	14.98%	10	Continuum removal spectral (647 nm)	4.43%
2	PCA1	13.67%	11	First-order derivative spectral(724 nm)	3.58%
3	SR2	12.39%	12	First-order derivative spectral(634 nm)	3.29%
4	Second-order derivative spectral(647 nm)	9.44%	13	TVI	3.16%
5	NDVI	8.56%	14	PRI	0.11%
6	SR1	8.01%	15	Second-order derivative spectral(714 nm)	0.00%
7	Reflectance (734 nm)	7.18%	16	Continuum removal spectral (714 nm)	0.00%
8	Reflectance (714 nm)	6.54%	17	Continuum removal spectral (734 nm)	0.00%
9	First-order derivative spectral(704 nm)	4.68%			

each of the six data sources to display its images, and the results are shown in Fig. 6.

3.3. Plant species classification results of 4 datasets

The four hyperspectral datasets described in Section 2.4.1 were used to identify plant species with the four classifiers described in Section 2.4.3. The classification accuracy results are shown in Table 5.

Dataset 3 was composed of reflectance images without feature transformation, and we used its classification result as a reference. For Dataset 4, the classification accuracy using RF, ANN, and SAM methods were higher than Dataset 3, and Dataset4 using ANN had the highest OA of 95.08% (kappa = 0.94). Thus, those bands after feature transformation effectively improved the accuracy of plant species classification, although the effectiveness may be affected or weakened by the classifier's ability to process high-dimensional data. For Dataset 1, the classification accuracies using the RF and SAM methods were higher than that of Dataset 3. RF had the highest performance among the four classifiers with an overall accuracy of 94.57% and kappa coefficient of 0.93. The classification accuracies of Dataset 1 and Dataset 2 were close to, or in some cases, higher than the accuracies when using Dataset3. Therefore, these selected bands by using Mahalanobis distance and variable importance evaluation based on the RF model performed well for plant species identification even though it had far fewer bands.

The grass distribution map for SVM, RF, ANN, and SAM methods applied to Dataset 1 at 0.65 mm resolution are shown in Figs. 7(a) and 7 (b).
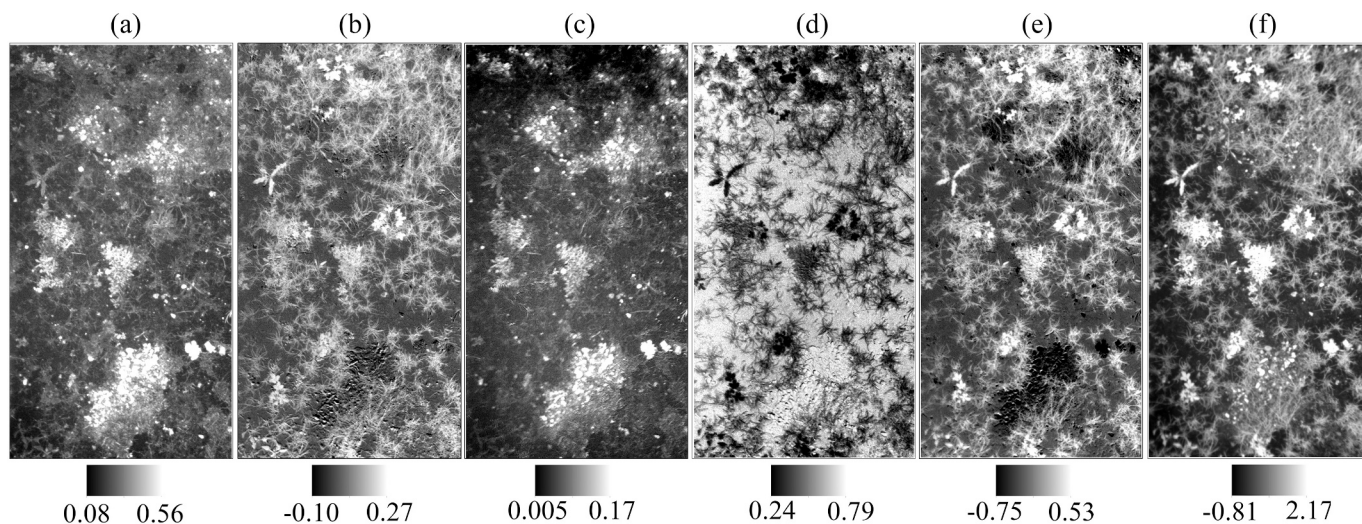

Fig. 6. Six types of variables. (a) Reflectance (647 nm), (b)First-order derivative spectral(704 nm), (c) Second-order derivative spectral(647 nm), (d)Continuum removal spectral(647 nm), (e) SR2, (f) PCA1.

Table 5
Accuracy for the four datasets.

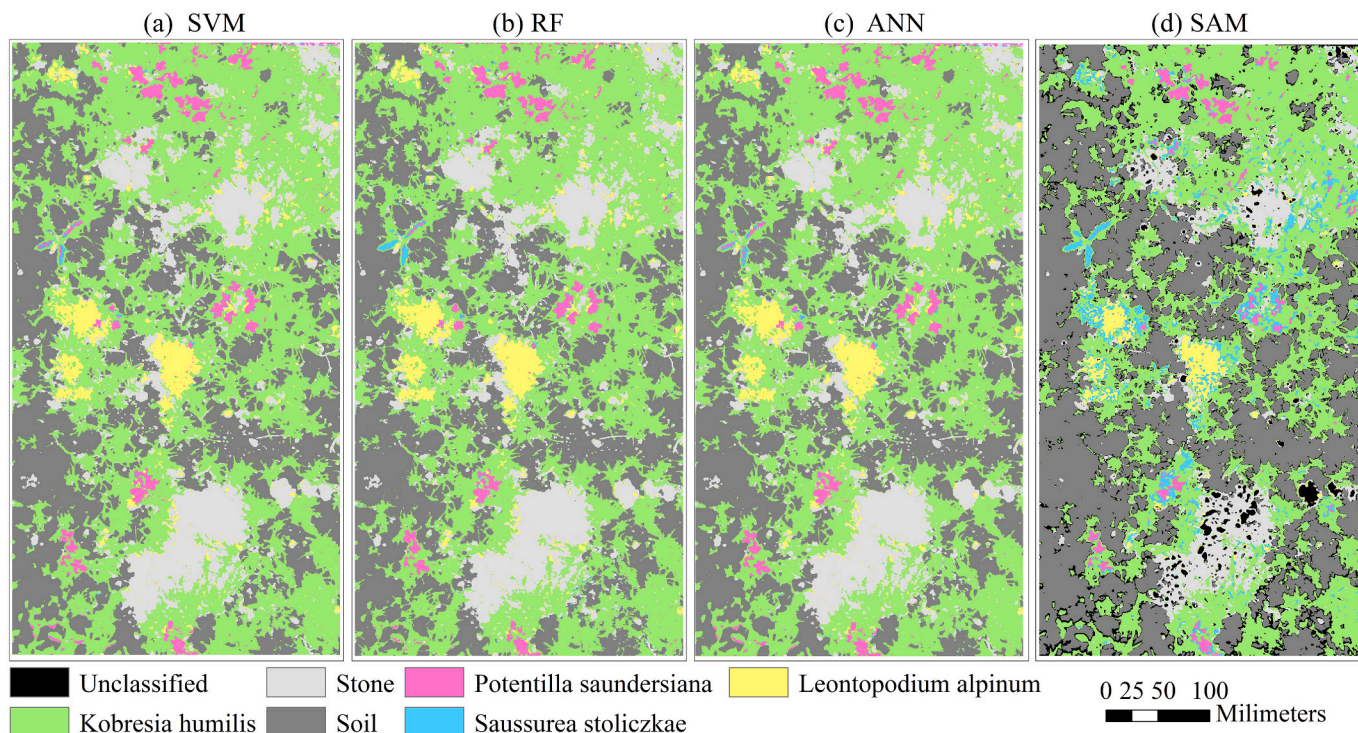|	Number of bands	SVM		RF		ANN		SAM	
		Kappa	OA	Kappa	OA	Kappa	OA	Kappa	OA
Dataset1	10	0.86	88.63%	0.931	94.57%	0.89	91.59%	0.74	78.71%
Dataset 2	17	0.89	92.13%	0.92	93.61%	0.90	92.66%	0.77	80.98%
Dataset 3	39	0.91	92.96%	0.93	94.34%	0.93	94.73%	0.69	74.84%
Dataset 4	171	0.82	86.05%	0.93	94.56%	0.94	95.08%	0.75	79.98%

Fig. 7. SVM, RF, ANN, and SAM classification results based on Dataset 1.

4. Discussion

4.1. Applicability of close-range hyperspectral for plant species identification

Presently, the two main types of remote sensing images used for plant species identification are hyperspectral imagery and UAV multispectral images. Some studies have identified invasive plant species and noxious weeds using field hyperspectral data (measured by HR-1024 or ASD) resampled to relatively low spatial resolution imagery, such as HJ-1A/HIS or AISA Eagle images (Mansour et al. 2012; Ai et al. 2020). Lu et al. (2017) used UAV imagery to identify grassland species compositions. However, the accuracy of plant species identification achieved by past work does not exceed 88.64% (Mansour et al. 2012).

Our classifications exceeded an accuracy of 91% using the four datasets and the SVM, RF, and ANN methods, even though the spectral resolution of the hyperspectral imager we used was lower than that of the ASD spectrometer, and the spectral range was narrower than that of the ASD spectrometer. These accuracies indicated that a spectral resolution of 10 nm and a spectral range of 400–900 nm were sufficient to identify the plant species in our study.

The classification accuracies from our results relied **on the high spatial resolution of close-range hyperspectral images**. Considering the characteristics of grasses in Northern Tibet, the spatial resolution of remote sensing images is an important factor for the identification of plant species. The spatial resolution of our close-range hyperspectral images was (0.65 mm) greater than the width of Kobresia humilis leaves, which had the thinnest leaves (about 3.5–5 mm) of the four plant species, so these leaves were clearly identified and this spatial resolution formed a foundation for the identification of plant species at the level of individuals.

The limitation of our experiment was that the close-range imaging camera acquired hyperspectral images of small areas. But our findings can provide guidance for further research on the identification of alpine plants species at larger spatial and temporal scales.

Table 6
The contribution of the six data sources and corresponding variables.

	Data sources	Variables	Contribution	Total contribution
1	Spectral indices	SR2	12.39%	32.22%
		NDVI	8.56%	
		SR1	8.01%	
		TVI	3.16%	
		PRI	0.11%	
2	Reflectance	647 nm	14.98%	28.7%
		734 nm	7.18%	
		714 nm	6.54%	
3	First principal component	PC1	13.67%	13.67%
4	First derivative	704 nm	4.68%	11.54%
		724 nm	3.58%	
		634 nm	3.29%	
5	Second order derivative	647 nm	9.44%	9.44%
		714 nm	0.00%	
6	Continuum removal spectral	647 nm	4.43%	4.43%
		714 nm	0.00%	0.00%
		734 nm	0.00%	0.00%

4.2. Effectiveness of the selected spectral bands and indicators

Eleven bands were selected from 156 bands based on the Mahalanobis distance. The wavelengths of 647 nm and 634 nm belong to the red band, while the wavelengths of 704 nm, 714 nm, 724 nm, and 734 nm belong to the red-edge bands. In the selection results, the red bands appeared three times, and the red edge bands appeared seven times, which indicated that these two bands were important for identifying the plant species. This result is consistent with the conclusions by Liu et al. (2013), who found that the positioning of a red edge reflects differences in the main vegetation types found in alpine meadows.

The contribution of the above six data sources and corresponding variables based on the variable importance evaluation method was shown in Table 6. Spectral indices were the most important data sources for classification results (especially SR) and were thus central to identifying the plant species in our study. The continuum removal spectra
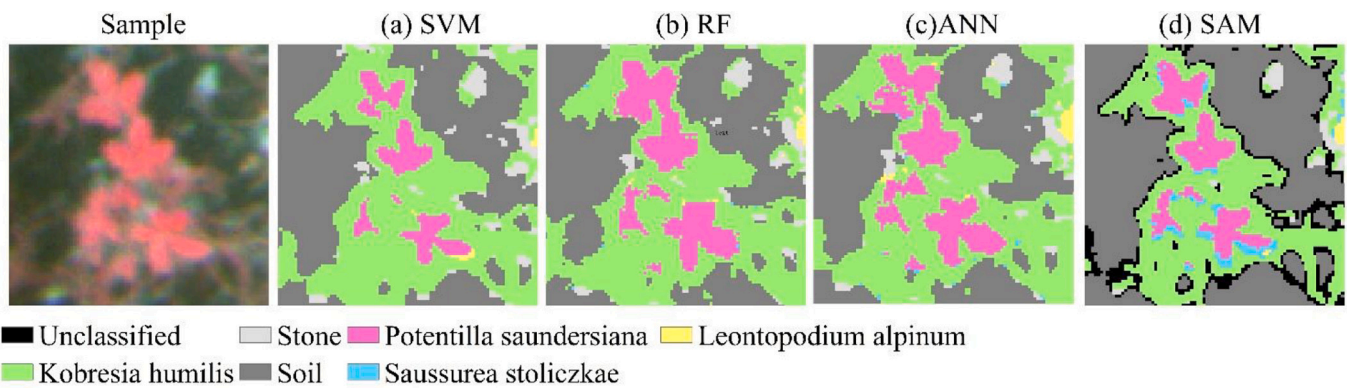
Fig. 8. A locally enlarged view of a false color image. (a), (b), (c) and (d) are the SVM, RF, ANN, and SAM classification results, respectively.

contributed the least to grass species identification. Differences in the chlorophyll content, cell structures, and water content of different plant species directly affect the spectral indices. The simple ratio (SR) vegetation index compares peaks in absorption and reflection caused by chlorophyll. George et al. (2019) found that the simple ratio correlates strongly with chlorophyll. Liu et al. (2013) found that indices that fully describe chlorophyll absorption characteristics and cellulose absorption features can better distinguish plant species, which may be the reason why SR (including SR2 and SR1) contributed so much to our classification results.

The selection results based on the Mahalanobis distance method and the variable importance evaluation method showed that the red bands, red edge bands, and spectral indices are important variables for grass species identification.

4.3. Effects of mapping algorithms on image classification

Among the four classifiers, RF and ANN performed well, with an OA of more than 91.60%, and the kappa coefficient was above 0.89. SAM performed the worst, with an average OA of 78.63% (kappa = 0.74) for the four datasets.

The classification accuracy of the four classifiers varied with the number of features used. Based on the RF method, the classification accuracies of the four datasets were all more than 93%. RF yielded an average classification accuracy of 94.27% (Kappa = 0.93) for the four datasets, which was better than the performance of the other three classifiers. For the ANN method, the highest effectiveness was achieved with more bands. The ANN map produced the highest overall accuracy when dealing with high-dimensional data (Dataset 4), with an overall accuracy of 95.08% and a kappa of 0.938. The classification accuracy of SVM was significantly reduced when processing high-dimensional data. The classification results of the four datasets using the SAM method showed that the classification accuracy of Dataset 3 was the lowest with an OA of 74.84% (kappa = 0.69). The overall performance of ANN was better than SVM and SAM, which was consistent with the results reported by Shaharum et al. (2018).

Locally enlarged views of the reflectance image and its classification results reveal more differences (Fig. 8). For *Potentilla saundersiana,* RF and ANN performed well at identification. However, SVM incorrectly classified some *Potentilla saundersiana* pixels as *Leontopodium pusillum,* and SAM classified some *Potentilla saundersiana* pixels as *Saussurea stoliczkae.*

It should be noted that SVM and ANN classifiers can be subdivided into many different types, and their performance may differ. Also, the number of decision trees in the RF algorithm, the type of kernel function used in SVM, the activation function and the number of hidden layers in the ANN algorithm, and the maximum angle threshold of the SAM will affect the classification results. The classification performances of these classifiers may generally depend on the number of samples, data types,

and specific research objectives (Cao et al. 2018).

5. Conclusion

Here, we explored different methods of identifying plant species of an alpine steppe using a close-range hyperspectral remote sensing image that we acquired from Naqu in Tibet, China. We analyzed the spectral characteristics between the different plant species, the importance of the spectral bands for plant species identification, and the effectiveness of the classifiers. First, we found that bands selected using the Mahalanobis distance and variable importance evaluation method showed that the red bands, red edge bands, and spectral indices were important for plant species identification. Second, the classification accuracy of the four classifiers varied with the number of features used. Among the four classifiers, the ANN classifier had the highest overall classification accuracy on Dataset 3 of reflectance images, which was 94.73%, and the Kappa coefficient was 0.93. Third, the machine learning algorithms RF and ANN performed well for identifying plant species, with overall accuracies of more than 91.59% and kappa coefficient above 0.89. Based on the RF method, the classification accuracies of the four datasets were all more than 93%. Our results suggest that close-range hyperspectral image and machine-learning classifiers, such as RF and ANN, can be used to effectively identify plant species in alpine steppe.

Our results provide the foundation needed for further research on the identification of alpine plants species and the analysis of grassland community structures at larger spatial and temporal scales. The insights gained from the implementation of our methods in future studies will provide vital information on the detection of alpine grassland degradation and the progress of ecological restoration.

Declaration of Competing Interest

No potential conflict of interest was reported by the authors.

Acknowledgments

References

Ai, Zetian, An, Ru, Lu, Caihong, Chen, Yuehong, 2020. Mapping of native plant species and noxious weeds to investigate grassland degradation in the Three-River Headwaters region using HJ-1A/HSI imagery. Int. J. Remote Sens. 41 (5), 1813–1838. https://doi.org/10.1080/01431161.2019.1675324.
Amlekar, M.M., Gaikwad, A.T., 2019. Plant classification using image processing and neural network. In: Balas, V., Sharma, N., Chakrabarti, A. (Eds.), Data Management,

Analytics and Innovation. Advances in Intelligent Systems and Computing, vol 839. Springer, Singapore. https://doi.org/10.1007/978-981-13-1274-8-29.

Arsa, Dewa Made Sri, Sanabila, Hadaiq Rolis, Rachmadi, M. Febrian, Gamal, Ahmad, Jatmiko, Wisnu, 2018. Improving Principal Component Analysis Performance for Reducing Spectral Dimension in Hyperspectral Image Classification. In: Paper presented at the 2018 International Workshop on Big Data and Information Security (IWBIS), Jakarta. https://doi.org/10.1109/IWBIS.2018.8471705. May 8-9.

Atkinson, Anthony C., Riani, Marco, 2014. Stalactite Plot. Wiley StatsRef, pp. 1–4. https://doi.org/10.1002/9781118445112.stat00412.pub2. Statistics Reference Online.

Belgiu, Mariana, Drăguţ, Lucian, 2016. Random forest in remote sensing: a review of applications and future directions. ISPRS J. Photogramm. Remote Sens. 114, 24–31. https://doi.org/10.1016/j.isprsjprs.2016.01.011.

Blackburn, George Alan, 1998. Spectral indices for estimating photosynthetic pigment concentrations: a test using senescent tree leaves. Int. J. Remote Sens. 19 (4), 657–675. https://doi.org/10.1080/014311698215919.

Brereton, Richard G., 2015. The chi squared and multinormal distributions. J. Chemom. 29 (1), 9–12. https://doi.org/10.1002/cem.2680.

Broge, N.H., Leblanc, E., 2001. Comparing prediction power and stability of broadband and hyperspectral vegetation indices for estimation of green leaf area index and canopy chlorophyll density. Remote Sens. Environ. 76 (2), 156–172. https://doi.org/10.1016/S0034-4257(00)00197-8.

Cao, Jingjing, Liu, Kai, Liu, Lin, Zhu, Yuanhui, Li, Jun, He, Zhi, 2018. Identifying Mangrove Species Using Field Close-Range Snapshot Hyperspectral Imaging and Machine-Learning Techniques. Remote Sens. 10 (12) https://doi.org/10.3390/rs10122047.

Celleri, Carla, Zapperi, Georgina, Trilla, Gabriela González, Pratolongo, Paula, 2019. Assessing the capability of broadband indices derived from Landsat 8 Operational Land Imager to monitor above ground biomass and salinity in semiarid saline environments of the Bahía Blanca Estuary, Argentina. Int. J. Remote Sens. 40 (12), 4817–4838. https://doi.org/10.1080/01431161.2019.1574992.

Chen, Bin, Li, HaiDong, Cao, XueZhang, 2014a. Advances in studies on degradation and re-vegetation of typical ecosystems on Tibetan Plateau, China. World Forest. Res. 27 (5), 18–23. https://doi.org/10.13348/j.cnki.sjlyyj.2014.05.004.

Chen, Baoxiong, Zhang, Xianzhou, Tao, Jian, Wu, Jianshuang, Wang, Jingsheng, Shi, Peili, Zhang, Yangjian, Chengqun, Yu., 2014b. The impact of climate change and anthropogenic activities on alpine grassland over the Qinghai-Tibet Plateau. Agric. For. Meteorol. 189, 11–18. https://doi.org/10.1016/j.agrformet.2014.01.002.

Cui, Xuefeng, Graf, Hans-F, 2009. Recent land cover changes on the Tibetan Plateau: a review. Clim. Chang. 94 (1–2), 47–61. https://doi.org/10.1007/s10584-009-9556-8.

Cui, Shi-chao, Ke-fa, Zhou, Ru-fu, Ding, 2019. Extraction of plant abnormal information in mining area based on hyperspectral. Spectrosc. Spectr. Anal. 39 (1), 241–249. https://doi.org/10.3964/j.issn.1000-0593(2019)01-0241-09.

Cushnahan, T.A., Yule, I.J., Pullanagari, R., Grafton, M.C.E., 2016. Identifying plant species using hyperspectral sensing. In: Currie, L.D., Singh, R. (Eds.), Integrated Nutrient and Water Management for Sustainable farming. CRC Press, Palmerston North. https://doi.org/10.1201/9780367803216.

Deng, Lai-fei, Fei, Zhang, Hai-wei, Zhang, Xian-long, Zhang, Jie, Yuan, 2019. Analysis of the spectral characteristics of Haloxylon Ammodendron under water stress. Spectrosc. Spectr. Anal. 39 (1), 210–215.

Din, Mairaj, Zheng, Wen, Rashid, Muhammad, Wang, Shanqin, Shi, Zhihua, 2017. Evaluating hyperspectral vegetation indices for leaf area index estimation of *Oryza sativa* L. at diverse phenological stages. Front. Plant Sci. 8, 820. https://doi.org/10.3389/fpls.2017.00820.

Ding, MingJun, Zhang, YiLi, Sun, XiaoMin, Liu, LinShan, Wang, ZhaoFeng, Bai, WanQi, 2013. Spatiotemporal variation in alpine grassland phenology in the Qinghai-Tibetan Plateau from 1999 to 2009. Chin. Sci. Bull. 58 (3), 396–405. https://doi.org/10.1007/s11434-012-5407-5.

Dong, Shikui, Shang, Zhanhuan, Gao, Jixi, Boone, Randall B., 2020. Enhancing sustainability of grassland ecosystems through ecological restoration and grazing management in an era of climate change on Qinghai-Tibetan Plateau. Agric. Ecosyst. Environ. 287, 106684 https://doi.org/10.1016/j.agee.2019.106684.

Driss, S.B., Soua, M., Kachouri, R., Akil, M., 2017. A comparison study between MLP and convolutional neural network models for character recognition. In: Real-Time Image and Video Processing 2017. International Society for Optics and Photonics. https://doi.org/10.1117/12.2262589, 10223: 1022306.

Feng, Wei, Qi, Shuangli, Heng, Yarong, Zhou, Yi, Wu, Yapeng, Liu, Wandai, He, Li, Li, Xiao, 2017. Canopy vegetation indices from in situ hyperspectral data to assess plant water status of winter wheat under powdery mildew stress. Front. Plant Sci. 8, 1219. https://doi.org/10.3389/fpls.2017.01219.

Fisher, Ryan J., Sawa, Ben, Prieto, Beatriz, 2018. A novel technique using LiDAR to identify native-dominated and tame-dominated grasslands in Canada. Remote Sens. Environ. 218, 201–206. https://doi.org/10.1016/j.rse.2018.10.003.

Gamon, J.A., Serrano, L., Surfus, J.S., 1997. The photochemical reflectance index: an optical indicator of photosynthetic radiation use efficiency across species, functional types, and nutrient levels. Oecologia 112 (4), 492–501. https://doi.org/10.2307/4221805.

Gao, Lin, Wang, Xiaofei, Johnson, Brian Alan, Tian, Qingjiu, Yu, Wang, Verrelst, Jochem, Xihan, Mu, Xingfa, Gu., 2020. Remote sensing algorithms for estimation of fractional vegetation cover using pure vegetation index values: a review. ISPRS J. Photogramm. Remote Sens. 159, 364–377. https://doi.org/10.1016/j.isprsjprs.2019.11.018.

George, Rajee, Hitendra, Padalia, Sinha, S.K., Senthil Kumar, A., 2019. Evaluating sensitivity of hyperspectral indices for estimating mangrove chlorophyll in Middle Andaman Island, India. Environ. Monit. Assess. 191 (3), 785. https://doi.org/10.1007/s10661-019-7679-6.

Harris, Richard B., Samberg, Leah H., Yeh, Emily T., Smith, Andrew T., Wenying, Wang, Junbang, Wang, 2016. Rangeland responses to pastoralists' grazing management on a Tibetan steppe grassland, Qinghai Province, China. Rangeland J. 38 (1), 1–15. https://doi.org/10.1071/RJ15040.

Huete, Alfredo R., 2012. Vegetation indices, remote sensing and forest monitoring. Geogr. Compass 6 (9), 513–532. https://doi.org/10.1111/j.1749-8198.2012. 00507.x.

Hughes, Gordon, 1968. On the mean accuracy of statistical pattern recognizers. IEEE Trans. Inf. Theory 14 (1), 55–63. https://doi.org/10.1109/TIT.1968.1054102.

Ishida, Tetsuro, Kurihara, Junichi, Viray, Fra Angelico, Namuco, Shielo Baes, Paringit, Enrico C., Perez, Gay Jane, Takahashi, Yukihiro, Marciano, Joel Joseph, 2018. A novel approach for vegetation classification using UAV-based hyperspectral imaging. Comput. Electron. Agric. 144, 80–85. https://doi.org/10.1016/j.compag.2017.11.027.

Izzuddin, M.A., Nisfariza, Mohd Noor, Ezzati, Bahrom, Idris, Abu Seman, Steven, Michael D., Boyd, Doreen, 2018. Analysis of airborne hyperspectral image using vegetation indices, red edge position and continuum removal for detection of ganoderma disease in oil palm. J. Oil Palm Res. 30 (3), 416–428. https://doi.org/10.21894/jopr.2018.0037.

Jordan, Carl F., 1969. Derivation of leaf-area index from quality of light on the forest floor. Ecology 50 (4), 663–666. https://doi.org/10.2307/1936256.

Kemp, David R., Guodong, Han, Xiangyang, Hou, Michalk, David L., Fujiang, Hou, Wu, Jianping, Yingjun, Zhang, 2013. Innovative grassland management systems for environmental and livelihood benefits. Proc. Natl. Acad. Sci. 110 (21), 8369–8374. https://doi.org/10.1073/pnas.1208063110.

Kopeć, Dominik, Zakrzewska, Agata, Halladin-Dąbrowska, Anna, Wylazłowska, Justyna, Kania, Adam, Niedzielko, Jan, 2019. Using airborne hyperspectral imaging spectroscopy to accurately monitor invasive and expansive herb plants: limitations and requirements of the method. Sensors 19 (13), 2871. https://doi.org/10.3390/s19132871.

Kuching, S., 2007. The performance of maximum likelihood, spectral angle mapper, neural network and decision tree classifiers in hyperspectral image analysis. J. Comput. Sci. 3 (6), 419–423. https://doi.org/10.3844/jcssp.2007.419.423.

Lehnert, Lukas W., Meyer, Hanna, Meyer, Nele, Reudenbach, Christoph, Bendix, Jörg, 2013. Assessing pasture quality and degradation status using hyperspectral imaging: a case study from western Tibet. In: Paper presented at the Remote Sensing for Agriculture, Ecosystems, and Hydrology XV. https://doi.org/10.1117/12.2028348, 88870.

Liang, Liang, Qin, Zhihao, Zhao, Shuhe, Di, Liping, Zhang, Chao, Deng, Meixia, Lin, Hui, Zhang, Lianpeng, Wang, Lijuan, Liu, Zhixiao, 2016. Estimating crop chlorophyll content with hyperspectral vegetation indices and the hybrid inversion method. Int. J. Remote Sens. 37 (13), 2923–2949. https://doi.org/10.1080/01431161.2016.1186850.

Lichtenthaler, Hartmut K., Gitelson, Anatoly, Lang, Michael, 1996. Non-destructive determination of chlorophyll content of leaves of a green and an aurea mutant of tobacco by reflectance measurements. J. Plant Physiol. 148 (3–4), 483–493. https://doi.org/10.1016/S0176-1617(96)80283-5.

Liu, Min, Liang, Rongling, Cao, Yongbin, 2015. Number of trees in random forest. Comp. Eng. Applications. 51 (5), 126–131. https://doi.org/10.3778/j.issn.1002-8331.1401-0264.

Liu, Bo, Wei-shou, S.H.E.N., Ru, L.I., Zhao-ping, Y.A.N.G., Nai-feng, L.I.N., 2013. Spectral characteristics of alpine grassland during degradation process in the source region of Yarlung Zangbo. Spectrosc. Spectr. Anal. 33 (6), 1598–1602. https://doi.org/10.3964/j.issn.1000-0593(2013)06-1598-05.

Lopatin, Javier, Fassnacht, Fabian E., Kattenborn, Teja, Schmidtlein, Sebastian, 2017. Mapping plant species in mixed grassland communities using close range imaging spectroscopy. Remote Sens. Environ. 201, 12–23. https://doi.org/10.1016/j.rse.2017.08.031.

Lu, Bing, He, Yuhong, 2017. Species classification using Unmanned Aerial Vehicle (UAV)-acquired high spatial resolution imagery in a heterogeneous grassland. ISPRS J. Photogramm. Remote Sens. 128, 73–85. https://doi.org/10.1016/j.isprsjprs.2017.03.011.

Lu, Jingshan, Yang, Tiancheng, Xi, Su, Qi, Hao, Yao, Xia, Cheng, Tao, Zhu, Yan, Cao, Weixing, Tian, Yongchao, 2019. Monitoring leaf potassium content using hyperspectral vegetation indices in rice leaves. Precis. Agric. https://doi.org/10.1007/s11119-019-09670-w.

Luo, Shanjun, He, Yingbin, Wang, Zhuozhuo, Duan, Dingding, Zhang, Jingke, Zhang, Yuantao, Zhu, Yaqiu, Yu, Jinkuan, Zhang, Shengli, Fei, Xu., 2019. Comparison of the retrieving precision of potato leaf area index derived from several vegetation indices and spectral parameters of the continuum removal method. Eur. J. Remote Sensing 52 (1), 155–168. https://doi.org/10.1080/22797254.2019.1572460.

Ma, X.F., Chen, S.Y., Deng, J., Feng, Q.S., Huang, X.D., 2016. Vegetation phenology dynamics and its response to climate change on the Tibetan Plateau. Acta Prataculturae Sinica 25 (1), 13–21. https://doi.org/10.11686/cyxb2015089.

Mahalanobis Chandra, Prasanta, 1936. On the generalised distance in statistics. Proceedings of the National Institute of Sciences of India 2 (1), 49–55.

Mansour, Khalid, Mutanga, Onisimo, Everson, Terry, Adam, Elhadi, 2012. Discriminating indicator plant species for rangeland degradation assessment using hyperspectral data resampled to AISA Eagle resolution. ISPRS J. Photogramm. Remote Sens. 70, 56–65. https://doi.org/10.1016/j.isprsjprs.2012.03.006.

Menze, Bjoern H., Michael Kelm, B., Masuch, Ralf, Himmelreich, Uwe, Bachert, Peter, Petrich, Wolfgang, Hamprecht, Fred A., 2009. A comparison of random forest and its Gini importance with standard chemometric methods for the feature selection and classification of spectral data. BMC Bioinform. 10 (1), 213. https://doi.org/10.1186/1471-2105-10-213.

Mishra, P., Asaari, M.S.M., Herrero-Langreo, A., et al., 2017. Close range hyperspectral imaging of plants: a review. Biosyst. Eng. 164, 49–67. https://doi.org/10.1016/j.biosystemseng.2017.09.009.

Monteiro, Sildomar T., Uto, Kuniaki, Kosugi, Yukio, Oda, Kunio, Iino, Yoshiyuki, Saito, Genya, 2008. Hyperspectral image classification of plant species in northeast Japan. In: Paper presented at the IGARSS 2008-2008 IEEE international geoscience and remote sensing symposium. Boston, MA, USA. https://doi.org/10.1109/IGARSS.2008.4779742.

Pal, Mahesh, Foody, Giles M., 2010. Feature selection for classification of hyperspectral data by SVM. IEEE Trans. Geosci. Remote Sens. 48 (5), 2297–2307. https://doi.org/10.1109/TGRS.2009.2039484.

Pasqualotto, Nieves, Delegido, Jesús, Van Wittenberghe, Shari, Verrelst, Jochem, Rivera, Juan Pablo, Moreno, José, 2018. Remote Estimation of Canopy Water Content in Different Crop Types with New Hyperspectral Indices. In: Paper presented at the IGARSS 2018–2018 IEEE International Geoscience and Remote Sensing Symposium, Valencia, Jul 23–27. https://doi.org/10.1109/IGARSS.2018.8517523.

Prasad, Thenkabail, 2011. Hyperspectral vegetation indices. Hyperspectral remote sensing of vegetation. CRC Press.

Qu, Yufu, Liu, Ziyue, 2017. Dimensionality reduction and derivative spectral feature optimization for hyperspectral target recognition. Optik 130, 1349–1357. https://doi.org/10.1016/j.ijleo.2016.11.143.

Rouse, J.W., Haas, R.H., Schell, J.A., Deering, D.W., 1974. Monitoring vegetation systems in the Great Plains with ERTS. In: Freden, Stanley C., Mercanti, Enrico P. (Eds.), Third Earth Resources Technology Satellite-1 Symposium. National Aeronautics and Space Administration, Greenbelt, pp. 301–317.

Sabat-Tomala, Anita, Raczko, Edwin, Zagajewski, Bogdan, 2020. Comparison of support vector machine and random Forest algorithms for invasive and expansive species classification using airborne hyperspectral data. Remote Sens. 12 (3), 516. https://doi.org/10.3390/rs12030516.

Schmidt, K.S., Skidmore, A.K., 2001. Exploring spectral discrimination of plant species in African rangelands. Int. J. Remote Sens. 22 (17), 3421–3434. https://doi.org/10.1080/01431160152609245.

Shaharum, N.S.N., Shafri, H.Z.M., Gambo, J., Abidin, F.A.Z., 2018. Mapping of Krau Wildlife Reserve (KWR) protected area using Landsat 8 and supervised classification algorithms. In: Remote Sensing Applications: Society and Environment, 10, pp. 24–35. https://doi.org/10.1016/j.rsase.2018.01.002.

Sun, Jian, Zhang, Zhenchao, Dong, Shikui, 2019. Adaptive management of alpine grassland ecosystems over Tibetan Plateau. Pratacultural Sci. 36, 933–938. https://doi.org/10.11829/j.issn.1001-0629.2019-0224.

Tan, Changwei, Wang, Dunliang, Zhou, Jian, Ying, Du, Luo, Ming, Zhang, Yongjian, Guo, Wenshan, 2018. Remotely assessing fraction of photosynthetically active radiation (FPAR) for wheat canopies based on hyperspectral vegetation indexes. Front. Plant Sci. 9, 776. https://doi.org/10.3389/fpls.2018.00776.

Tucker, Compton J., 1978. Red and photographic infrared linear combinations for monitoring vegetation. Remote Sens. Environ. 8, 127–150. https://doi.org/10.1016/0034-4257(79)90013-0.

Wang, Haizhu, Guo, Wenxin, Zhao, Ruifeng, Zhou, Bo, Chao, Hu., 2018. A real-time online security situation prediction algorithm for power network based on Adaboost and SVM. In: Paper presented at the International Conference on Security with Intelligent Computing and Big-data Services, April 6-7. https://doi.org/10.1007/978-3-030-16946-6_42.

Xiao, Q., Li, G., Xie, L., Chen, Q., 2018. Real-world plant species identification based on deep convolutional neural networks and visual attention. Ecol. Informatics 48, 117–124. https://doi.org/10.1016/j.ecoinf.2018.09.001.

Xu, Kai-jian, Tian, Qing-jiu, Xu, Nian-xu, Yue, Ji-bo, Tang, Shao-fei, 2019. Classifying Forest dominant trees species based on high dimensional time-series NDVI data and differential transform methods. Spectrosc. Spectr. Anal. 39 (12), 3794–3800. https://doi.org/10.3964/j.issn.1000-0593(2019)12-3794-07.

Yao, Xixi, Wu, Jianping, Gong, Xuyin, Lang, Xia, Wang, Cailian, Song, Shuzhen, Ahmad, Anum Ali, 2019. Effects of long-term fencing on biomass, coverage, density, biodiversity and nutritional values of vegetation community in an alpine meadow of the Qinghai-Tibet Plateau. Ecol. Eng. 130, 80–93. https://doi.org/10.1016/j.ecoleng.2019.01.016.

Zhang, Dong, Zhang, Fei, 2014. Application of fractional differential in preprocessing hyperspectral data of saline soil. Trans. Chin. Soc. Agric. Eng. 30 (24), 151–160. https://doi.org/10.3969/j.issn.1002-6819.2014.24.018.

Zhang, F., Zhou, G., 2019. Estimation of vegetation water content using hyperspectral vegetation indices: a comparison of crop water indicators in response to water stress treatments for summer maize. BMC Ecol. 19 (1), 18. https://doi.org/10.1186/s12898-019-0233-0.

Zakrani, abdelali, Hain, Mustapha, Namir, Abdelwahed, 2019. Investigating the use of random forest in software effort estimation. Procedia computer science 148, 343–352. https://doi.org/10.1016/j.procs.2019.01.042.

Zhang, Yuxiang, Bo, Du, Zhang, Liangpei, Wang, Shugen, 2015. A low-rank and sparse matrix decomposition-based Mahalanobis distance method for hyperspectral anomaly detection. IEEE Trans. Geosci. Remote Sens. 54 (3), 1376–1389. https://doi.org/10.1109/TGRS.2015.2479299.

Zhao, Xinquan, Zhao, Liang, Li, Qi, Chen, Huai, Zhou, Huakun, Xu, Shixiao, Dong, Quanmin, Wu, Gaolin, He, Yixin, 2018. Using balance of seasonal herbage supply and demand to inform sustainable grassland management on the Qinghai-Tibetan Plateau. Front. Agric. Sci. Eng. 5 (1), 1–8. https://doi.org/10.15302/J-FASE-2018203.